nature communications

Article

https://doi.org/10.1038/s41467-024-53196-3

Logarithmic and Archimedean organic crystalline spirals

Received: 19 June 2024

Accepted: 4 October 2024

Published online: 18 October 2024

Check for updates

Xuesong Yang[1], Linfeng Lan[1], Ibrahim Tahir[2], Zainab Alhaddad[2], Qi Di[1], Liang Li[2,3], Baolei Tang[1] ✉, Panče Naumov[2,4,5,6] ✉ & Hongyu Zhang[1] ✉

Crystals can be found in many shapes but do not usually grow as spirals. Here we show that applying a non-uniform layer of a polymer blend onto slender centimeter-size organic crystals prestrains the crystals into hybrid dynamic elements with spiral shapes that respond reversibly to environmental variations in temperature or humidity by curling. Exposure to humidity results in partial uncurling within several seconds, whereby a logarithmic-type spiral crystal is transformed into an Archimedean one. Conical helices obtained by lateral pulling of the spirals can wind around solid objects similar to plant tendrils or lift suspended objects with a positive correlation between the actuator's elongation and the cargo mass. The morphological, kinematic, and kinetic attributes turn these hybrid materials into an attractive platform for flexible sensors and soft robots, while they also provide an approach to morph crystalline fibers in non-natural spiral habits inaccessible with the common crystallization approaches.

When confronted with complex, extreme, or changing environments, biological organisms usually respond with adaptation[1–12]. The remarkable adaptability allows the organisms to alleviate the detrimental effects of specific external conditions and ultimately survive. The kinematic principles of the motility associated with the adaptive aspects of the natural world can be translated into the materials' realm to create intelligent systems that circumvent the limited lifetime and diversify the applications of some traditionally used materials. Notable progress has been made in this scientific pursuit, with dynamic organic crystals garnering widespread attention in soft robotics[13–16]. Initially, the interest in dynamic molecular crystals was driven by the intention to design lightweight organic actuators, and subsequent prolific research work revealed that crystals of photochemically active organic compounds can exhibit an array of behaviors such as bending, curling, twisting, crawling, and jumping[17–27]. Among the basic deformation modes available with slender dynamic crystals, bending is the most common deformation, followed by twisting, while curling is not commonly encountered because it requires very long crystals capable of acute bending; the common platy crystals are known to curl only slightly. Despite many proven assets, the limited durability, specific chemical structures, and single operational mode of the organic crystals currently appear to impede their viability as dynamic materials for soft robots. Recent examples of the combination of dynamic organic crystals with polymers and the advent of polymer-crystal hybrid materials that capitalize on the assets of two materials classes provide means to overcome these challenges[28–31]. A remarkable instance of curling from nature is the mechanism used by the butterflies that extend their sucking mouthpart (proboscis) to feed from flowers (Fig. 1a)[32]. The proboscis is normally curled up, but it is uncurled to reach nutrients through a remote or narrow space in the flower. Drawing inspiration from the sophisticated curling mechanism of the proboscis and similar curling one-dimensional biogenic structures, we have designed a class of highly adaptable, curling hybrid spiral crystalline actuators in this study. The unconventional shape and kinematics of these actuating elements, together with their short response time and capability to respond to both temperature and humidity, expand the portfolio of the currently available shapes and deformations with dynamic crystals. It also points to the hybridization of organic crystals with other material

[1]State Key Laboratory of Supramolecular Structure and Materials, College of Chemistry, Jilin University, Changchun, P. R. China. [2]Smart Materials Lab, New York University Abu Dhabi, Abu Dhabi, United Arab Emirates. [3]Department of Sciences and Engineering, Sorbonne University Abu Dhabi, Abu Dhabi, UAE. [4]Center for Smart Engineering Materials, New York University Abu Dhabi, Abu Dhabi, UAE. [5]Research Center for Environment and Materials, Macedonian Academy of Sciences and Arts, Bul. Krste Misirkov 2, Skopje, Macedonia. [6]Molecular Design Institute, Department of Chemistry, New York University, 100 Washington Square East, New York, NY, USA. ✉e-mail: tangbl15@mails.jlu.edu.cn; pance.naumov@nyu.edu; hongyuzhang@jlu.edu.cn

https://doi.org/10.1038/s41467-024-53196-3

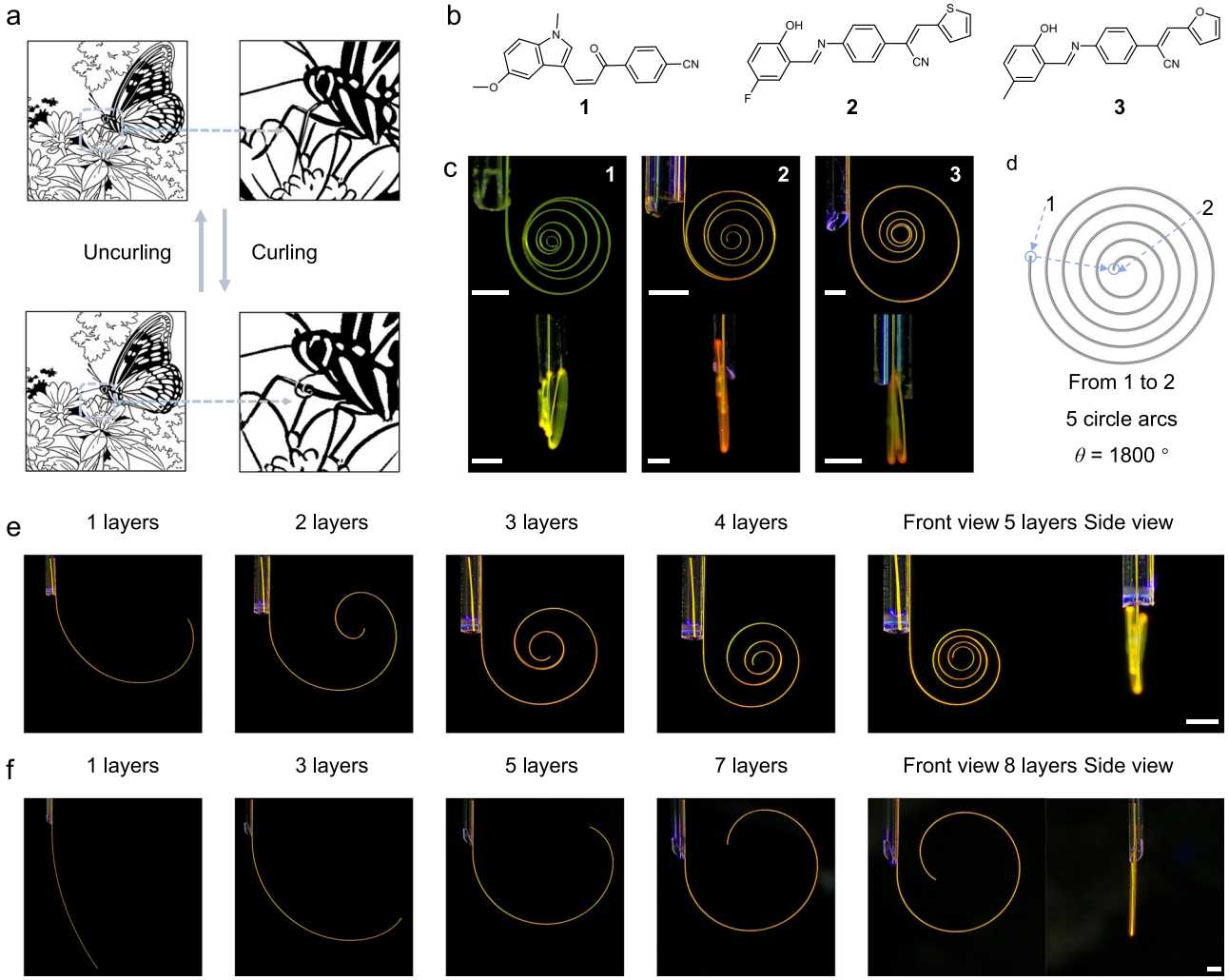

Fig. 1 | Concept and preparation of hybrid crystalline spirals. a Schematic illustration of the mechanism used by butterflies to feed from flowers in nature using their proboscis. **b** Chemical structures of the elastic crystals **1**–**3**. **c** Photos of the hybrid crystals P^4//**1**–**3** curling at low humidity (*RH* = 11.7%). The images were taken under UV light for enhanced contrast against the background. The upper and lower figures show the front and side views, respectively. **d** Diagram showing the method used to calculate the angle of a curled hybrid crystal. **e**, **f** Dependence of the degree of curling of two P^4//**2** hybrid crystals on the number of PVA/PSS layers. Scale bars, 400 μm.

classes as a roadmap to circumvent their natural limitations while capitalizing on their flexibility and structural order.

Results

Preparation of the hybrid organic crystals

Inspired by the curling and uncurling of some biological systems, we developed binary hybrid actuating elements based on flexible organic crystals that consist of two main components: supportive and active. Centimeter–length slender elastic crystals of three chemically different organic compounds (**1**–**3** in Fig. 1b and Supplementary Figs. 1–3) were selected as mechanically supportive components[28,30,33]. These crystals are very elastic and can be bent repeatedly into a U-shape without breaking (Supplementary Fig. 4 and Supplementary Table 1). The surfaces of **1**–**3** were first coated with a mixture of poly(diallyldimethylammonium) (PDDA) and poly(styrene 4-sulfonate) (PSS) to obtain $(PDDA/PSS)_5$//**1**–**3** (Supplementary Fig. 5). Subsequently, using a needle tip, small droplets of a mixture of polyvinyl alcohol (PVA) and PSS were deposited as the active component (Supplementary Fig. 6) along one of the bendable facets of the crystals, affording hybrid materials described as PVA/PSS//PDDA/PSS//**1**–**3**, or P^4//**1**–**3** for short (Fig. 1c). After drying, the polymer layer firmly adhered to the crystals, and the hybrid elements were mechanically compact. PVA is a commonly used hygroscopic polymer with a low critical solution temperature that is known to readily swell by the formation of hydrogen bonds. Since the polymer was coated on only one of the two wide faces of the crystal, differential strain is generated when the polymer contracts, which translates into a bending moment that causes the crystal to undergo macroscopic curling (Supplementary Fig. 7). As shown in Supplementary Fig. 8, PVA/PSS polymer was deposited on different wide surfaces of the organic crystal, and the hybrid material can curl clockwise or anti-clockwise when the humidity is decreased. In addition, by changing the position of PVA/PSS deposited on the surface of organic crystals, the hybrid material can be bent into different shapes (Supplementary Fig. 9). These hybrid polymer crystals can be curled into a spiral by applying multiple layers of PVA/PSS (Supplementary Fig. 10). Figure 1d shows an ideal spiral model with five circle arcs from point 1 to point 2, equivalent to 1800°, and depicts a convention that is used hereafter to describe the spiraling. As shown in Fig. 1e, f, the curvature, and therefore, the number of arc circles of P^4//**2**, increases with the number of layers of PVA/PSS when the relative humidity (*RH*) is maintained constant (*RH* = 11.3%). The thickness of the polymer layer affects the stiffness of the structure; for example, P^4//**2** curled four circle arcs when it had five layers of PVA/PSS (Fig. 1e) but only one circle when it had eight layers (Fig. 1f). Organic

https://doi.org/10.1038/s41467-024-53196-3

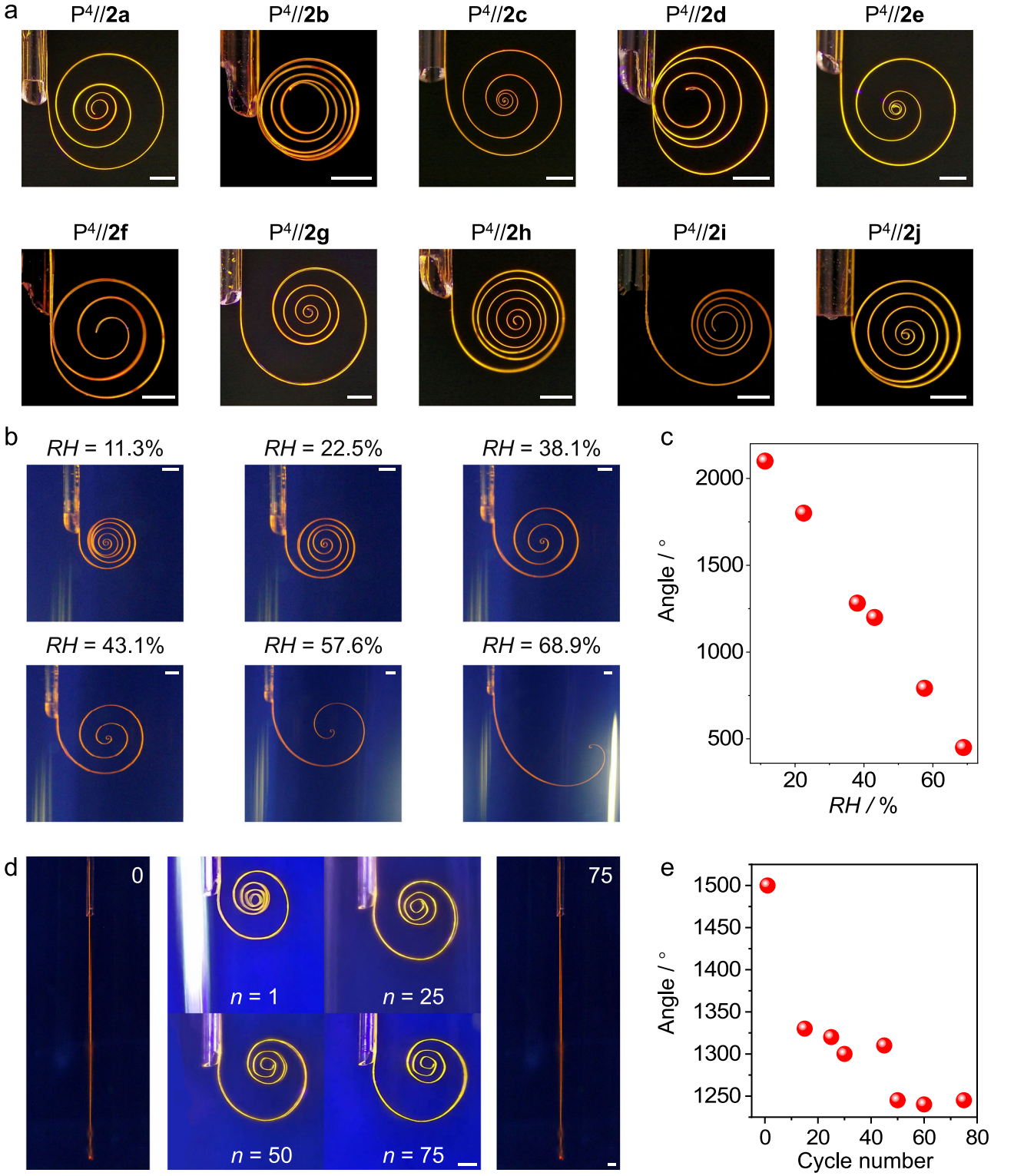

Fig. 2 | Humidity sensing and cyclability of the hybrid crystalline spirals. **a** Photographs of ten hybrids P[4]//**2** of different sizes (P[4]//**2a**–P[4]//**2j**) that curl to a different degree at a constant humidity of *RH* = 11.3%. **b** Curling of P[4]//**2** at different relative humidity (*RH*) levels at 25 °C. **c** Curling angle of P[4]//**2**, as defined in Fig. 1d, plotted as function of humidity (linear fit: $y = -29x + 2422°$). **d** Cyclability of P[4]//**2** over 75 cycles between two relative humidity points (*RH* = 66.1% and 22.5%). **e** Variation of the curling angle of P[4]//**2** with the cycle number. Scale bars, 400 μm.

crystals offer unique advantages as mechanically reinforcing components. Their highly ordered molecular arrangement provides favorable mechanical properties while maintaining light weight, and the properties of organic crystals can be tuned through molecular design and crystal engineering, offering a wide range of possibilities for customizing the properties of the resulting hybrid materials.

Response of the hybrid organic crystals to stimuli

Ten hybrid crystals of different sizes (P[4]//**2a**–P[4]//**2j** in Fig. 2a) were chosen to study the contributing factors among the size, degree of curling, and the number of PVA/PSS layers (Supplementary Table 2). The hybrid elements were more prone to curling when the crystal was thinner, wider, and longer, and the coated PVA/PSS was thicker

(Supplementary Fig. 3). For example, both P⁴//**2 f** and P⁴//**2 g** were coated with the same number of PVA/PSS layers, however, the latter curled more prominently because it was thinner and longer. P⁴//**2j** was thicker in size compared to P⁴//**2a** but curled more due to the thicker PVA/PSS layer. In addition, the diameter of the outermost circle (R_1) and the diameter of the innermost circle (R_2) for P⁴//**2c** were 0.22 cm and 0.01 cm, which are 12.8% and 0.3% of the length (L), respectively. This considerable reduction in length could be applied, for example, for actuation in small, flexible devices. Figure 2b shows that the curling angle of P⁴//**2** changes up to 2100° from *RH* = 68.9% to *RH* 11.3% (25 °C). In Supplementary Fig. 11, the degree of curling of crystals at different humidities was investigated by choosing saturated aqueous solutions of different salts. As shown in Fig. 2c, the curling angle decreases when the relative humidity increases. With the cyclability over long–term usage being the main prerequisite for actuation applications, an initially straight crystal of P⁴//**2** at *RH* = 84.3% was cycled 75 times between *RH* = 66.1% and *RH* = 22.5% (25 °C), and it returned to its straight shape at *RH* = 84.3% after the final cycle (Fig. 2d). This recovery occurred with 11.3% reduction in the curling angle after 15 cycles and 17.0% after 75 cycles (Fig. 2e). As shown in Supplementary Fig. 12, the surface of the hybrid organic crystals after multiple curling/straightening cycles was observed by scanning electron microscopy, and it was found that the coating was still uniformly distributed on the surface of the crystals. In order to investigate whether the length of the crystal changed after spiraling of the hybrid material has occurred, crystals of **2** and P⁴//**2** were compared and it was found that the length of P⁴//**2** did not change after spiraling (Supplementary Fig. 13). The single-crystal structures of the crystals before and after 100 deformations were characterized by single crystal X-ray diffraction, and the results indicated that the crystals remained crystalline and of good quality after multiple deformations (Supplementary Table 3).

Attaining high sensitivity is another important characteristic of the materials that are used in kinematic devices such as flexible actuators. The degree of curling and the actuation rate was investigated at different temperatures (Fig. 3a). Upon placement in a high-temperature environment, the hybrid crystals rapidly curled and formed a tight spiral due to the contraction of the polymer (Fig. 3a and Supplementary Movie 1). Upon rapid approach to a heated object (50 °C), the slightly curved P⁴//**2** rapidly bent to 2880° within 6.23 s. The curling velocity gradually decreased, from 1698° s^{-1} after the first 0.53 s to 361° s^{-1} after the 6.23 s of actuation (Fig. 3a). Upon removal of the hot object and cooling to 25 °C (*RH* = 66.3%), the actuator quickly uncurled from 2880° to 720° in 10.30 s, corresponding to a velocity of 370° s^{-1} after 0.73 s and 210° s^{-1} after 10.30 s of uncurling (Fig. 3b).

Applications of the hybrid organic crystals

The spiraling of the hybrid materials depends on external conditions, such as humidity and temperature (Figs. 2a and 3a). Visually and mechanistically, the crystals resemble a spring—a standard mechanical part whose elasticity is utilized for saving energy, measuring force, and vibration dampening. Inspired by this analogy, a small-scale model of a crane was constructed consisting of two parts that can lift an object by decreasing relative humidity (Fig. 4a). A cylindrical strip of paper (0.20 mg) and curled P⁴//**2**, which was fixed at one end (*RH* = 56.8%, *T* = 25 °C), were placed on a silicon wafer (step 1) (Fig. 4b and Supplementary Movie 2). When the humidity decreased, the actuator straightened and expanded through the cylinder (step 2). Upon decrease of humidity, the element curled, lifting the object 17 mm above the surface (steps 3–7). When the humidity increased rapidly, the element straightened, and the paper slid off onto the surface (step 8). This device weighs 0.02 mg and can lift firmly an 0.20 mg object, which is approximately ten times heavier. The spring elongates as the object gets heavier, and thus, its ability to lift cargo of different weights was tested. Five objects of various weights were lifted by the actuator while measuring the elongation (the distance between the highest and lowest points) under different humidity (Fig. 4c, d and Supplementary Fig. 14). The mass of the cargo and the elongation of the device were found to be positively correlated (Fig. 4e) at constant humidity (*RH* = 22.5%).

The control of spiral shape and deviation from the planarity of natural helical structures helps certain biological organisms to adjust and control their length, configuration, and helicity in various environments. By using a needle to mechanically pull its tip outwards, a planar spiral was transformed into a three-dimensional structure, a conical helix (Fig. 5a). Using the above method, P⁴//**2** was converted from a planar spiral into a conical helix at *RH* = 11.3%. The deformation was plastic, and the helix did not revert to the spiral shape, probably due to the plasticity of the polymer (Fig. 5b)[34]. As shown with the helix of P⁴//**2** (Supplementary Fig. 15), the helices can be pulled to have an arbitrary pitch (Fig. 5c), and their handedness can be changed by changing the direction from which the spiral is pulled (Fig. 5d, e, Supplementary Fig. 16 and Supplementary Movie 3). We further investigated if this transformation can be performed in a controlled manner. As shown in Supplementary Fig. 17, one end of the crystal was fixed, and the other end was glued to an embroidery needle attached to the arm of a universal testing machine. The setup was programmed to repeatedly move the needle vertically, 7 mm above and below the initial position. This action resulted in helices with either R or S configuration, demonstrating this method's reproducibility (Supplementary Movie 4). The plasticity in the deformation induced by stretching by using a needle is not unexpected since, unlike the in-plane bending that occurs by humidity-induced expansion, the pulling force likely induces defects in the interface between the two materials. Indeed, we observed that while upon application of smaller forces, the spiral shape is recovered, the application of stronger lateral forces or multiple acts of pulling results in permanent deformation into a helical shape (Supplementary Fig. 18 and Supplementary Movie 5). These experiments demonstrate the exceptional flexibility and configurational adjustability of the hybrid crystal-polymer spirals.

Discussion

The natural dynamic spiraling structures are ubiquitous, as beautifully illustrated by the curling of the elephant trunks that operate as muscular hydrostats[35], some animal tails[36], octopi's tentacles[37], and conch shells such as the brilliant shell of the pink conch[38]. In a monumental work, Cook studied the spiral's association with the phenomenon of life and astutely noted that a spiral is a curve of life[39]. At a molecular level, some of the essential biological macromolecules, such as proteins and nucleic acids, and most notably DNA, also form helices[40,41]. Many plants like petunias, wisterias, or passion flowers have developed tendrils to approach and climb objects, showcasing unique features that might inspire design (Fig. 6a). Figure 6b (Supplementary Movie 6) shows a simulation of the function of such tendrils with the curling hybrid crystals described above. To that end, a capillary glass tube was placed horizontally in front of P⁴//**2** (step 1). The end of P⁴//**2** was heated with a nitrile-gloved hand at a temperature of about 37 °C, as confirmed by thermal imaging (Supplementary Fig. 19), causing it to bend upwards and engulf the tube's front (step 2). The middle and end sections were then reheated, enabling bending downwards (step 3). Finally, upon heating of the entire structure, P⁴//**2** wound itself around the capillary glass tube (step 4). Upon removal of the nitrile gloved hand, P⁴//**2** returned to its initial state (steps 5–8). The series of steps were successfully reproduced with thicker objects, for example, by using two capillary glass tubes instead of one (Supplementary Movie 7).

Rolling is an efficient mode of movement seen in nature, enabling insects like the Moroccan flic-flac spider to swiftly evade threats by curling into a wheel-like shape and rolling sideways[42]. Inspired by the spider's motion, a helical object that is capable of controlled rolling was designed, as depicted in Fig. 6c. When placed on a slope, the object would remain stationary. However, when forced to curl, it would adopt a helical shape and roll down the slope (steps 1–4). The

https://doi.org/10.1038/s41467-024-53196-3

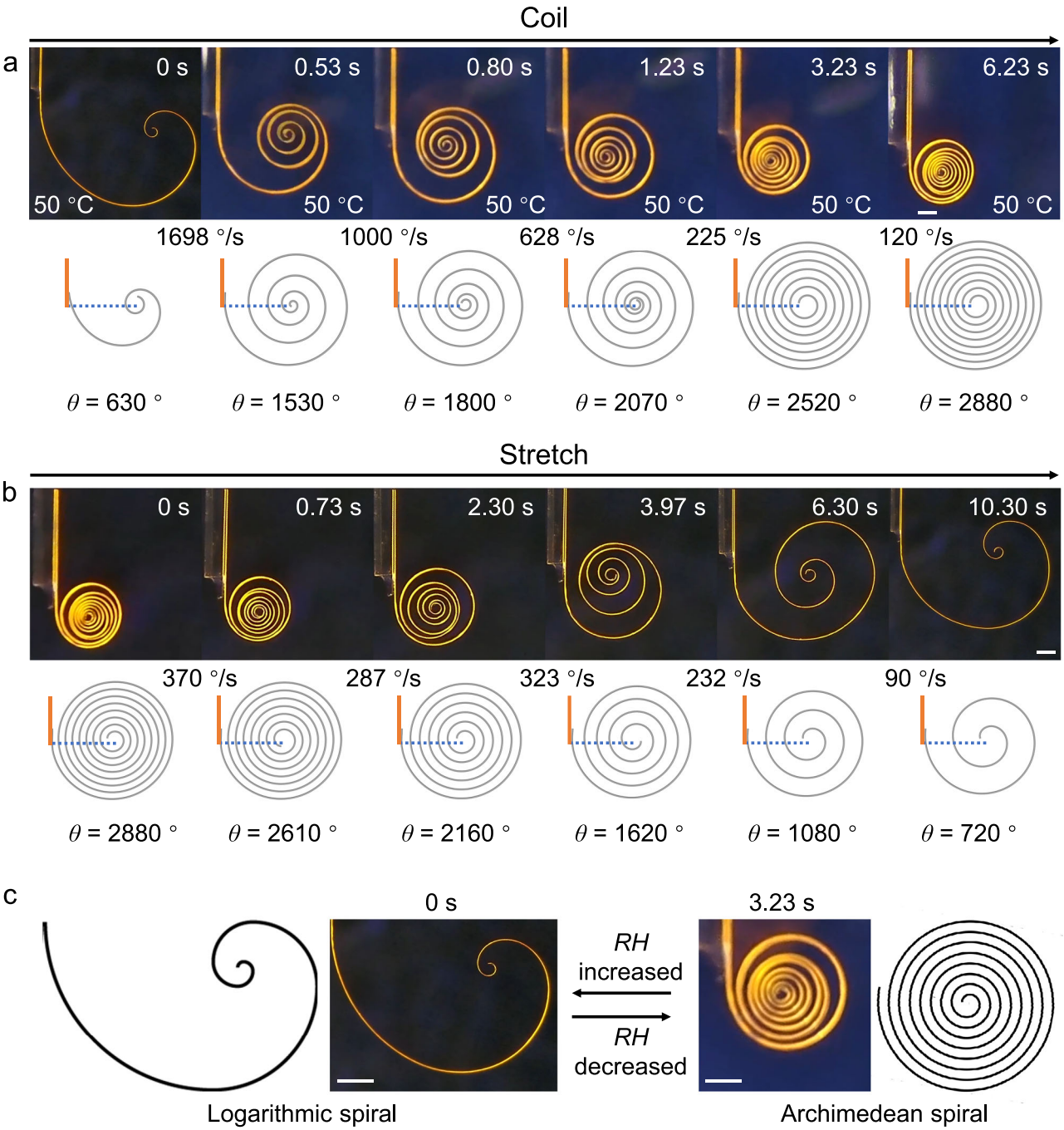

Fig. 3 | Actuation performance of the spiral hybrid actuators. a, **b** Photographs of a spiral actuator P[4]//**2** during its approach to (**a**) and removal away from (**b**) a glass object heated at 50 °C. **c** Change of the type of the spiral from logarithmic to Archimedean induced by change in humidity. Scale bars, 400 μm.

principles of this motion were realized with the hybrid crystals, as shown in Fig. 6d (Supplementary Movie 8). When placed on a silicon wafer inclined at 30°, the crystal remained motionless (step 1), but it curled and started rolling when it was approached by a nitrile-gloved finger (step 2). When the heat source was removed, the actuator gradually recovered its original shape, and stopped rolling (steps 3–5). The switching of the rolling motion was repeated until the actuator reached the base (steps 6–9). Similar to the adaptability of the octopi, known for their flexibility, the materials described here can deform to navigate diverse environments[43]. In Fig. 6e and Supplementary Movie 9, a hybrid crystal fixed on an embroidery needle moves through a 0.3 mm-wide glass capillary. Pulling the needle with forceps gradually transforms the crystal from a spiral to a linear shape, enabling its advancement inside the capillary (steps 1–5). Upon exiting the tube, the crystal reverts to its original spiral shape (steps 6–8).

Extensive research has analyzed and categorized common spiral structures, leading to the formulation of regular mathematical expressions, such as different mathematical types of spirals[44]. Motivated by the reproducibility in the shape of the hybrid crystals observed in this work, we attempted modeling these actuators by some of the common mathematical forms of a spiral. The spiral crystals of P[4]//**2** resemble two types of spirals, namely a logarithmic spiral and an Archimedean spiral[45]. The mathematical expression of an Archimedean spiral is given by Eq. (1):

$$r(\theta) = a + b\theta \tag{1}$$

https://doi.org/10.1038/s41467-024-53196-3

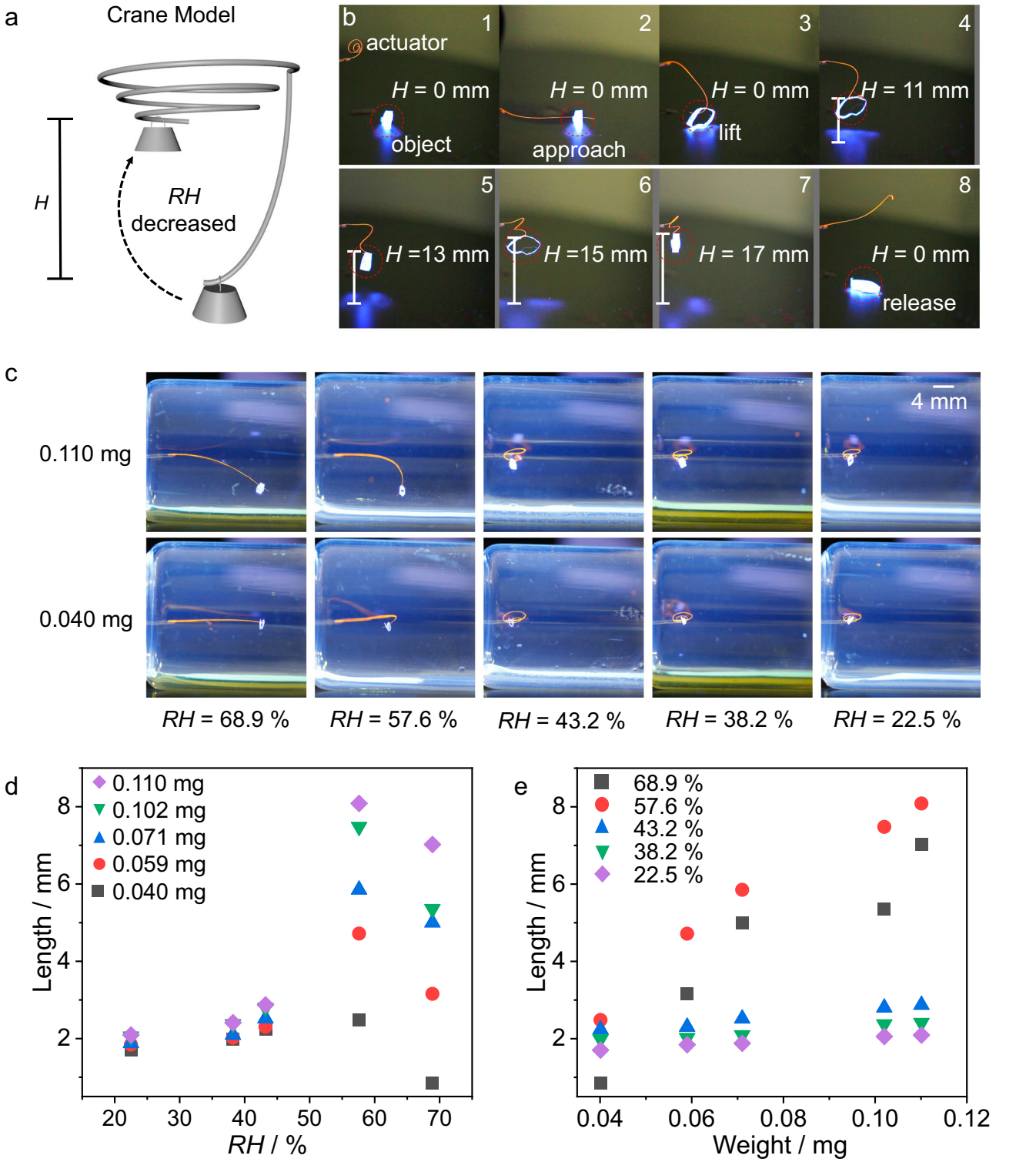

Fig. 4 | Performance of the spiral hybrid actuators when lifting objects. **a** Schematic diagram of a model of a crane based on the spiraling actuator of P^4//**2**. **b** Snapshots showing the actuator lifting an object. **c** The actuator lifts objects at different humidity levels. **d** Variation of the height with humidity measured for different weights of the cargo. **e** Variation of the height with weight of the cargo measured at different humidity levels.

while the logarithmic spiral is represented by Eq. (2):

$$r(\theta) = ae^{b\theta} \tag{2}$$

In Eqs. (1) and (2), r is the distance from the origin to a point on the curve, a is the initial distance from the origin to the starting point of the spiral, b is a constant determining how tightly the spiral winds and θ is the angle in radians (Fig. 7). The Archimedean spiral (Fig. 7a) exhibits a linear growth, where the distance from its center increases at a constant rate; each turn of the spiral maintains a consistent separation from the previous one[44]. The geometric structure of this spiral is characterized by a regular and straightforward increase in distance from the origin. In contrast, the logarithmic spiral (Fig. 7b) follows exponential growth, causing it to expand more rapidly with each

https://doi.org/10.1038/s41467-024-53196-3

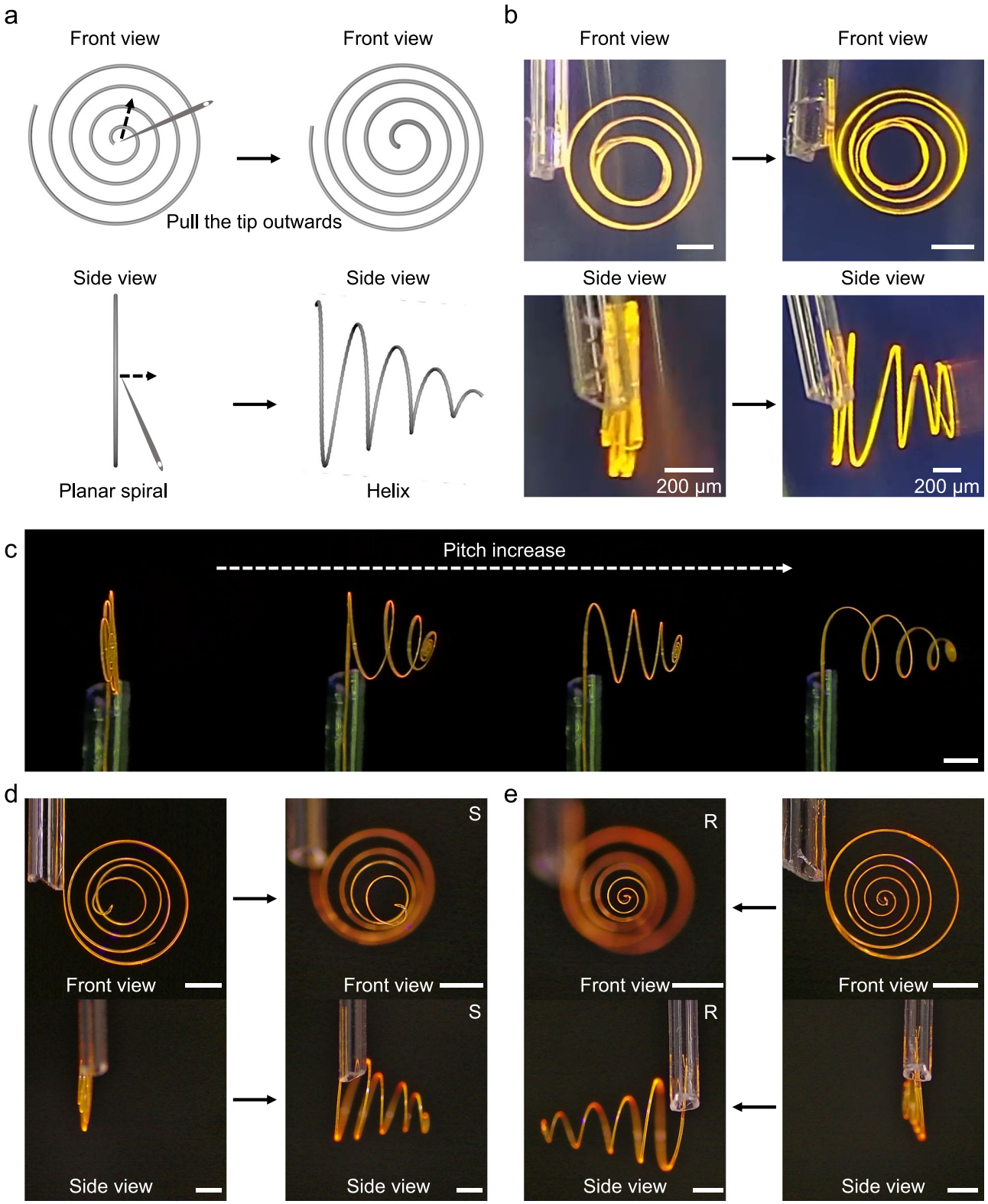

Fig. 5 | Spiral modulation of hybrid crystals. a Diagram of the transformation of a planar spiral into a spatial spiral. **b** An actuator being transformed from a planar spiral into a three-dimensional spiral (helix). **c** Adjustment of the pitch of the helix by using a needle to gradually pull its tip outward. **d**, **e** Hybrid crystalline helices with opposite handedness, left-handed (S, **d**) and right-handed (R, **e**). Scale bars, 400 μm.

revolution. It maintains a constant angle between the curve and its tangent, resulting in a self-similar property[45]. This means that as the spiral grows, its shape remains unaltered with each successive curve. The self-similarity of the logarithmic spiral is a distinctive feature, giving rise to other variations in shapes, such as golden spirals or Fibonacci spirals, special cases of spirals that have also been observed in nature[44,45].

As depicted in Fig. 3c, our experiments demonstrate that the hybrid material P^4//**2** reported here, with its remarkable sensitivity upon curling and stretching, can be structurally modified to behave

https://doi.org/10.1038/s41467-024-53196-3

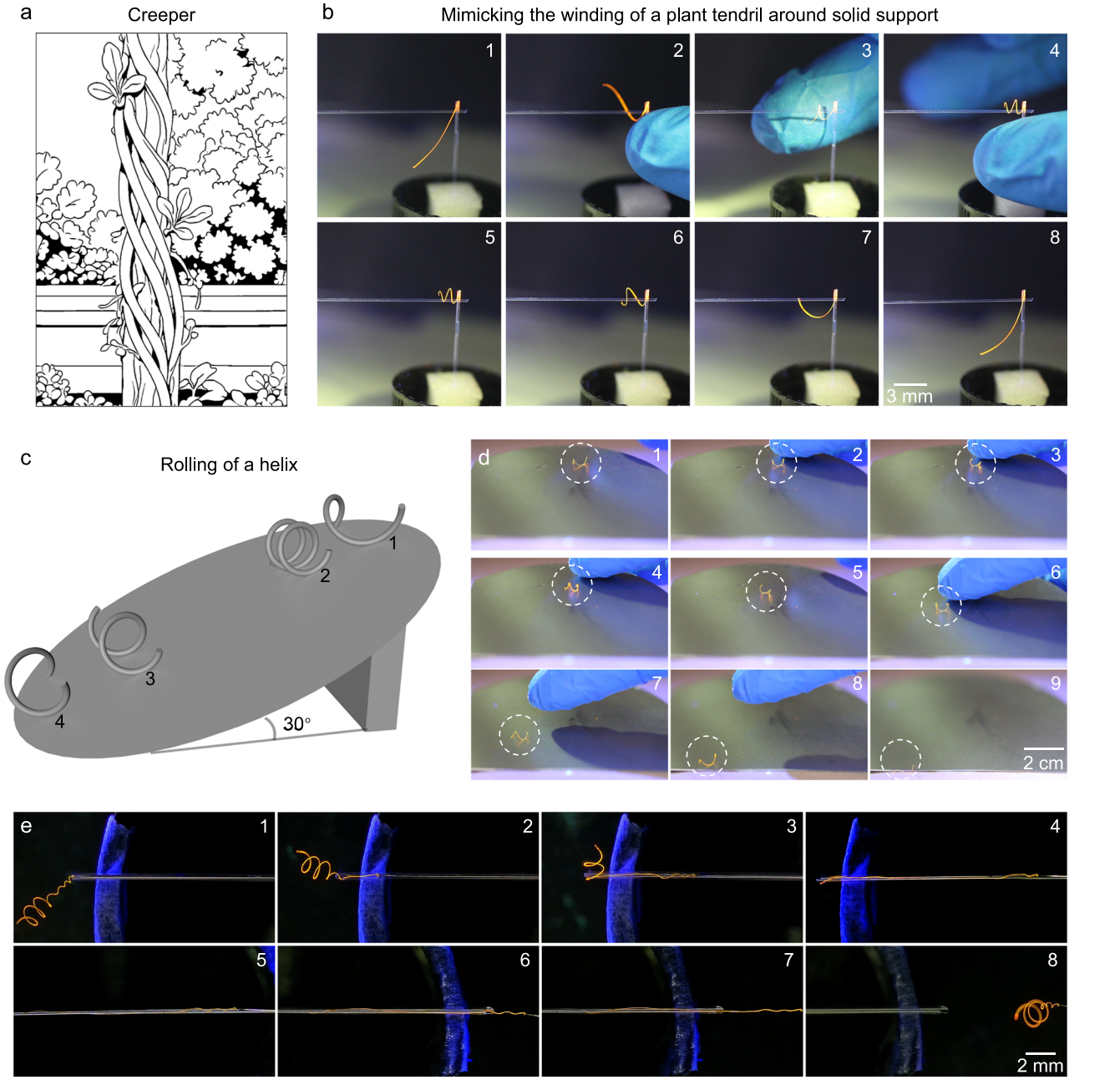

Fig. 6 | Biomimetic simulation of helical motions with artificial hybrid spirals and helices. a Examples of creepers that use tendrils for attachment to solid surfaces. **b** Photographs of a hybrid crystal actuator simulating the winding of a plant tendril. **c** Model of an object rolling. **d** An actuator curling into a wheel shape and rolling down a slope when heated with a nitrile-gloved finger. **e** Photographs of hybrid crystals crossing through the aperture.

like a logarithmic spiral or an Archimedean spiral by varying the thickness of the crystal, changing the number of PVA/PSS layers, or, alternatively, by using different relative humidity. As shown in Supplementary Fig. 20 (Supplementary Movie 10), P^4//**3** can also be converted from a logarithmic to an Archimedean spiral by heating and exposure to humidity, confirming that the general transformation from a spiral that approximates a logarithmic shape to the one that is closer to an Archimedean shape does not depend on the crystal structure. For example, the hybrid crystals P^4//**2e** and P^4//**2j** can be represented by a logarithmic function and an Archimedean function, respectively. Figure 7d shows a logarithmic function that fits the spiral shape of P^4//**2e**. This function is represented as:

$$r(\theta) = 0.36e^{0.19\theta}, 0 \le \theta \le 12\pi \quad (3)$$

Figure 7c shows an Archimedean function that reproduces well the shape of the hybrid crystal P^4//**2j**. In this case, the Archimedean function can be represented with the following equation:

$$r(\theta) = 0.4 - 1.2\theta, 0 \le \theta \le 10\pi \quad (4)$$

It is worth noting that the extracted function is not an absolute perfect fit of the crystal because there is a tendency for this crystal to shift from a logarithmic spiral to an Archimedean spiral; hence an absolute mathematical representation for each spiral will have to incorporate both functions. Interestingly, in some instances, the spiraling can be seen following the golden ratio (φ)[44]. This is the case with the crystal in Fig. 3c, where the spiraling can be represented as a

https://doi.org/10.1038/s41467-024-53196-3

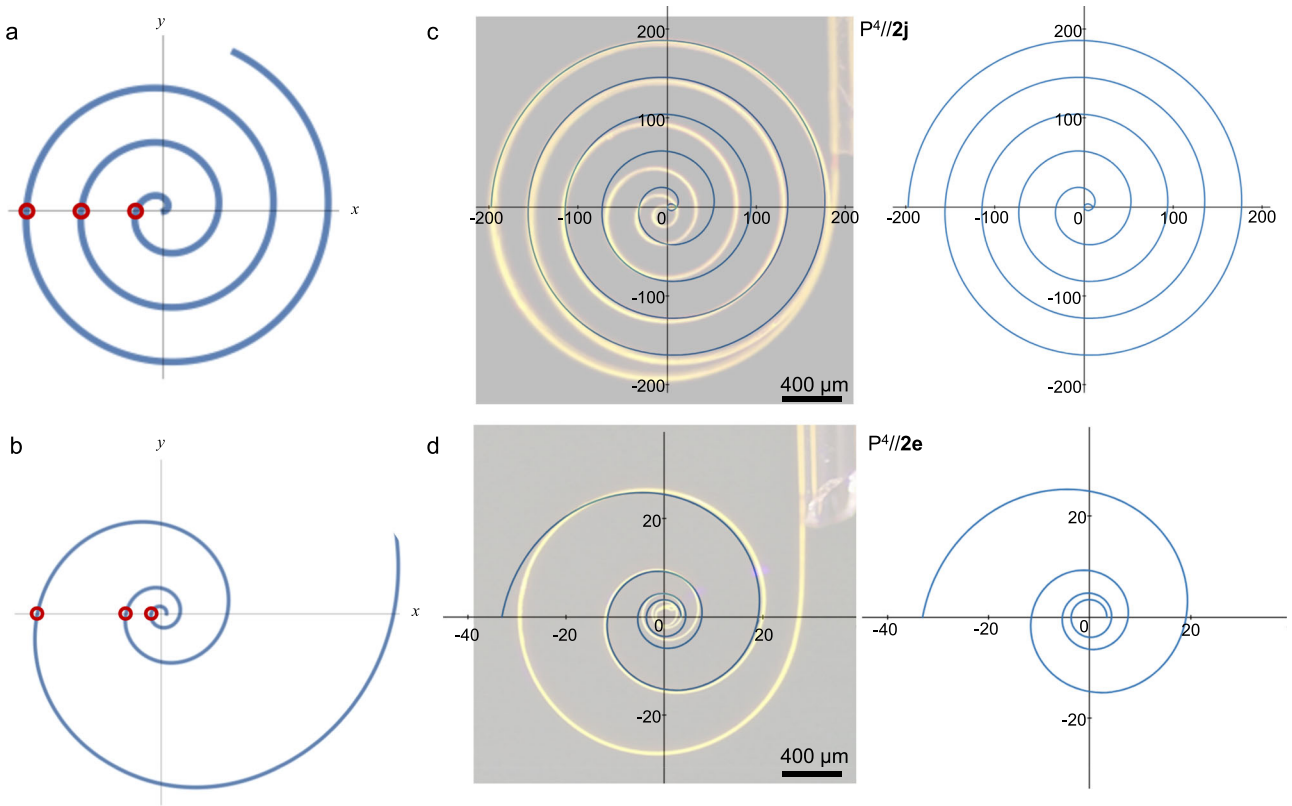

Fig. 7 | Modeling the curvature of the hybrid crystals to logarithmic and Archimedean functions. a A typical Archimedean spiral with red dots representing the constant distance between the adjacent intersections. **b** A typical logarithmic spiral with red dots representing logarithmic increase between every intersection along the *x* axis. **c** The Archimedean function that best fits the P^4//**2j** crystal. **d** The logarithmic function that best fits the P^4//**2e** crystal.

function of a golden spiral:

$$r = \varphi^{(2\theta/\pi)} \tag{5}$$

The golden spiral, a variant of the logarithmic spiral, is a curve traced out by a point moving with a constant angular velocity and increasing radial distance according to the Fibonacci series[46]. Fibonacci spirals are prevalent in nature, with the nautilus shell representing the quintessential classical example of the golden ratio[47,48]. In a remote analogy, the visual resemblance between the dynamic nature of this inanimate material and the fascinating functioning living systems mentioned above that have developed over the course of evolution is striking despite the fact that, both structurally and mechanistically, the hybrid material is very simple. This transition from a logarithmic-type spiral to an Archimedean one is not only of fundamental interest from a mechanical engineering perspective, but it also demonstrates the ability to control an unusual, non-natural morphology of a dynamic material. Such programmable geometric changes could be relevant to the conversion of linear to rotary or other motion in applications such as microfluidic valves, adaptive optics, and sensors. The geometric variation between different helical shapes could also amplify the effect of small environmental stimuli into much more prominent and more easily detectable responses, potentially increasing the sensitivity of some devices, such as, for example, flexible sensors.

In summary, we describe a new class of dynamic crystals—spiraling hybrid actuators that are based on a combination of organic crystal and polymer, where the mechanically coupled hygro/thermo-responsive polymer has an active function, while the organic crystal has a mechanically supportive role. This method for preparation of crystals with spiral shape is universal, and as shown by different organic crystals in this work, a variety of hybrids between organic crystals and polymers could be utilized to prepare crystals that curl with changes in heat, humidity, or light. By using different coating methods or by mechanical intervention, a planar spiral hybrid crystal can be converted into a three-dimensional spiral, that is, a conical helix. The degree and rate of curling were found to depend on a combination of factors, such as crystal size, humidity, and thickness of the polymer. This and other similar hybrid materials with other crystal-polymer combinations could be used as soft actuators to achieve complex motions. The results point to the opportunities to extend the application of adaptive organic crystals to flexible sensing, electronics, and bionics in the future.

Methods

Materials

All solvents and starting materials were purchased from commercial sources and used as received. Poly(diallyldimethylammonium chloride) (PDDA, M_w ca. 200,000–350,000), poly(styrene 4-sulfonate) (PSS, M_w ca. 70,000), polyvinyl alcohol (PVA, M_w ca. 105,000), were purchased from Energy Chemical. The aqueous solutions of PDDA and PSS were at a concentration of 1.0 mg mL^{-1}. To prepare the 5% PVA aqueous solution, PVA granules were mixed with pure water in PVA: H_2O = 5: 95 (w/w). The suspension was stirred at room temperature for 2 h and then at 95 °C in a water bath for an additional 2 h, affording a clear solution.

Preparation of compounds 1–3 and their crystals

The synthesis of compounds **1**–**3** is shown in Supplementary Figs. 1–3 (for characterization, see Supplementary Figs. 21–26). To prepare the crystals, saturated solutions of compounds **1**–**3** in dichloromethane were first added to separate test tubes. Subsequently, a triple volume

of ethanol was gently added along the walls of the test tubes without mixing. The test tubes were closed by using a sealing film, and after one to two weeks at room temperature, needle-like crystals of **1**–**3** were obtained.

Fabrication of the organic polymer-crystal hybrid materials P[4]//1–3

The long crystals were immersed in 1 mg mL^{-1} solution of poly(diallyldimethylammonium chloride) PDDA for 20 min, and rinsed with distilled water for 1 min. Then, they were immersed in 1 mg mL^{-1} solution of PSS for 20 min and rinsed with distilled water for 1 min. These steps were repeated to coat the crystals. By using a needle tip, a mixture of PVA and PSS was deposited on one of the crystal's wide faces. As the solvent evaporated at room temperature, a polymer film formed on the surface of the crystal, affording the hybrid crystals P[4]//**1**–**3**.

X-ray crystallographic analysis

Diffraction data of P[4]//**3** in its initial state and after 100 deformations were collected on a Rigaku RAXIS-PRID diffractometer. The data collection, integration, scaling, and absorption corrections were performed with the Bruker Apex 3 software[49]. The structures were solved with direct methods using Olex2[50] and refined by using the full-matrix least-squares method on F^2. The non-hydrogen atoms were refined anisotropically. The positions of the hydrogen atoms were calculated and refined isotropically. The program PLATON was used for the geometrical calculations[51]. The graphics related to the structures were generated by using Mercury 4.2.0[52]. Additional details of crystallographic data are provided in Supplementary Table 3.

Scanning electron microscopy (SEM)

The samples were mounted on a piece of carbon tape, and SEM images were obtained using high-vacuum mode on a FEI Quanta 450 field emission scanning electron microscope with a primary electron energy of 5–10 kV.

Data availability

The X-ray crystallographic coordinates for the structures reported in this study have been deposited at the Cambridge Crystallographic Data Centre (CCDC), under deposition number 2378281 for a crystal of P[4]//**3** in its initial state and 2378409 for a crystal of P[4]//**3** after 100 cycles of deformation. These data can be obtained free of charge from the Cambridge Crystallographic Data Centre via www.ccdc.cam.ac.uk/data_request/cif. The relevant data used in this study are available in the figshare database under accession code https://doi.org/10.6084/m9.figshare.27107107. Source data are provided in this paper.

References

1. Russell, E. S. Biological adaptedness and specialization of instinctive behaviour. *Nature* **147**, 729–734 (1941).
2. Lasker, G. W. Human biological adaptability. *Science* **166**, 1480–1486 (1969).
3. Brodeur, J. & McNeil, J. N. Seasonal microhabitat selection by an endoparasitoid through adaptive modification of host behavior. *Science* **244**, 226–228 (1989).
4. Wren, B. W. Microbial genome analysis: insights into virulence, host adaptation and evolution. *Nat. Rev. Genet.* **1**, 30–39 (2000).
5. Kowalski, C. H. et al. Fungal biofilm morphology impacts hypoxia fitness and disease progression. *Nat. Microbiol.* **4**, 2430–2441 (2019).
6. Mitchell, A. et al. Adaptive prediction of environmental changes by microorganisms. *Nature* **460**, 220–224 (2009).
7. Crowl, J. T. et al. Tissue-resident memory CD^{8+} T cells possess unique transcriptional, epigenetic and functional adaptations to different tissue environments. *Nat. Immunol.* **23**, 1121–1131 (2022).
8. Niu, Y., Sun, H. & Stevens, M. Plant camouflage: ecology, evolution, and implications. *Trends Ecol. Evol.* **33**, 608–618 (2018).
9. Bu, X. & Bai, H. Recent progress of bio-inspired camouflage materials: from visible to infrared range. *Chem. Res. Chin. Univ.* **39**, 19–29 (2023).
10. Liu, Z. et al. Thermo- and mechanochromic camouflage and self-healing in biomimetic soft actuators based on liquid crystal elastomers. *Angew. Chem. Int. Ed.* **61**, e202115755 (2022).
11. Nesher, N., Levy, G., Grasso, F. W. & Hochner, B. Self-recognition mechanism between skin and suckers prevents octopus arms from interfering with each other. *Curr. Biol.* **24**, 1271–1275 (2014).
12. Brackenbury, J. Caterpillar kinematics. *Nature* **390**, 453 (1997).
13. Naumov, P., Sahoo, S. C., Zakharov, B. A. & Boldyreva, E. V. Dynamic single crystals: kinematic analysis of photoinduced crystal jumping (the photosalient effect). *Angew. Chem. Int. Ed.* **52**, 9990–9995 (2013).
14. Sahoo, S. C., Panda, M. K., Nath, N. K. & Naumov, P. Biomimetic crystalline actuators: structure–kinematic aspects of the self-actuation and motility of thermosalient crystals. *J. Am. Chem. Soc.* **135**, 12241–12251 (2013).
15. Panda, M. K., Runčevski, T., Husain, A., Dinnebier, R. E. & Naumov, P. Perpetually self-propelling chiral single crystals. *J. Am. Chem. Soc.* **137**, 1895–1902 (2015).
16. Nath, N. K. et al. Model for photoinduced bending of slender molecular crystals. *J. Am. Chem. Soc.* **136**, 2757–2766 (2014).
17. Bushuyev, O. S., Singleton, T. A. & Barrett, C. J. Fast, Reversible, and general photomechanical motion in single crystals of various azo compounds using visible light. *Adv. Mater.* **25**, 1796–1800 (2013).
18. Zhu, L., Al-Kaysi, R. O. & Bardeen, C. J. Reversible photoinduced twisting of molecular crystal microribbons. *J. Am. Chem. Soc.* **133**, 12569–12575 (2011).
19. Kitagawa, D., Nishi, H. & Kobatake, S. Photoinduced twisting of a photochromic diarylethene crystal. *Angew. Chem. Int. Ed.* **52**, 9320–9322 (2013).
20. Uchida, E., Azumi, R. & Norikane, Y. Light-induced crawling of crystals on a glass surface. *Nat. Commun.* **6**, 7310 (2015).
21. Taniguchi, T. et al. Walking and rolling of crystals induced thermally by phase transition. *Nat. Commun.* **9**, 538 (2018).
22. Hean, D., Alde, L. G. & Wolf, M. O. Photosalient and thermosalient crystalline hemithioindigo-anthracene based isomeric photoswitches. *J. Mater. Chem. C* **9**, 6789–6795 (2021).
23. Gupta, P., Karothu, D. P., Ahmed, E., Naumov, P. & Nath, N. K. Thermally twistable, photobendable, elastically deformable, and self-healable soft crystals. *Angew. Chem. Int. Ed.* **57**, 8498–8502 (2018).
24. Skoko, Ž., Zamir, S., Naumov, P. & Bernstein, J. The thermosalient phenomenon. "Jumping crystals" and crystal chemistry of the anticholinergic agent oxitropium bromide. *J. Am. Chem. Soc.* **132**, 14191–14202 (2010).
25. Panda, M. K. et al. Strong and anomalous thermal expansion precedes the thermosalient effect in dynamic molecular crystals. *Sci. Rep.* **6**, 29610 (2016).
26. Klaser, T. et al. Does thermosalient effect have to concur with a polymorphic phase transition? The case of methscopolamine bromide. *Crystals* **8**, 301 (2018).
27. Ahmed, E. et al. Ultrafast, light, soft martensitic materials. *Adv. Funct. Mater.* **32**, 2112117 (2020).
28. Lan, L. et al. Hybrid elastic organic crystals that respond to aerial humidity. *Angew. Chem. Int. Ed.* **61**, e202200196 (2022).
29. Lan, L. et al. Organic single-crystal actuators and waveguides that operate at low temperatures. *Adv. Mater.* **34**, 2200471 (2022).
30. Yang, X. et al. Remote and precise control over morphology and motion of organic crystals by using magnetic field. *Nat. Commun.* **13**, 2322 (2022).

31. Yang, X. et al. Bioinspired soft robots based on organic polymer-crystal hybrid materials with response to temperature and humidity. *Nat. Commun.* **14**, 2287 (2023).
32. Lehnert, M. S. et al. Physical adaptations of butterfly proboscises enable feeding from narrow floral tubes. *Funct. Ecol.* **35**, 1925–1937 (2021).
33. Yang, X. et al. Electrically conductive hybrid organic crystals as flexible optical waveguides. *Nat. Commun.* **13**, 7874 (2022).
34. Jean, L. *Handbook of Materials Behavior Models*. 1179–1200 (Academic Press, 2001).
35. Longren, L. L. et al. Dense reconstruction of elephant trunk musculature. *Curr. Biol.* **33**, 4713–4720 (2023).
36. Massaro, L., Massa, F., Simpson, K., Fragaszy, D. & Visalberghi, E. The strategic role of the tail in maintaining balance while carrying a load bipedally in wild capuchins (*Sapajus libidinosus*): a pilot study. *Primates* **57**, 231–239 (2016).
37. Wang, T., Halder, U., Gribkova, E. & Gazzola, M. Modeling the neuromuscular control system of an octopus arm. Preprint at https://doi.org/10.48550/arXiv.2211.06767 (2022).
38. Hou, D. F., Zhou, G. S. & Zheng, M. Conch shell structure and its effect on mechanical behaviors. *Biomaterials* **25**, 751–756 (2004).
39. Cook, T. A. *The Curves of Life. Dover Publications* (1979).
40. Maffeo, C., Quednau, L., Wilson, J. & Aksimentiev, A. DNA double helix, a tiny electromotor. *Nat. Nanotechnol.* **18**, 238–242 (2023).
41. Manton, I. The spiral structure of chromosomes. *Biol. Rev.* **25**, 486–508 (1950).
42. Tan, N., Mohan, R. E. & Elangovan, K. Scorpio: A biomimetic reconfigurable rolling–crawling robot. *Int. J. Adv. Robot. Syst.* **13**, 1 (2016).
43. Finn, J. K., Tregenza, T. & Norman, M. D. Defensive tool use in a coconut-carrying octopus. *Curr. Biol.* **19**, 1069–1070 (2009).
44. Diedrichs, D. R. Archimedean, Logarithmic and Euler spirals – intriguing and ubiquitous patterns in nature. *Math. Gaz.* **103**, 52–64 (2019).
45. Polezhaev, A. in *Spirals and Vortices*. (2019).
46. Duan, J. Shrinkage points of golden rectangle, Fibonacci spirals, and golden spirals. *Discrete Dyn. Nat. Soc.* 3149602 (2019).
47. Schwerdtfeger, L. A. Spirals of science. *Science* **362**, 1318–1318 (2018).
48. Sasaki, N. et al. Supramolecular double-stranded Archimedean spirals and concentric toroids. *Nat. Commun.* **11**, 3578 (2020).
49. APEX3, v2015.52; Bruker AXS Inc.: Madison, WI (2015).
50. Dolomanov, O. V., Bourhis, L. J., Gildea, R. J., Howard, J. A. K. & Puschmann, H. OLEX2: A complete structure solution, refinement, and analysis program. *J. Appl. Crystallog.* **42**, 339–341 (2009).
51. Spek, A. L. Single-crystal structure validation with the program PLATON. *J. Appl. Crystallogr.* **36**, 7–13 (2003).
52. Macrae, C. F. et al. Mercury CSD 2.0-New features for the visualization and investigation of crystal structures. *J. Appl. Crystallogr.* **41**, 466–470 (2008).

Acknowledgements

This work was supported by the National Natural Science Foundation of China (52173164, 52373181, 523B2032), Natural Science Foundation of Jilin Province (20230101038JC), and a fund from New York University Abu Dhabi (P.N.). This material is based upon works supported by Tamkeen under NYUAD RRC Grant No. CG011 (P.N.).

Author contributions

X.Y., I.T., Z.A., L.Lan, B.T., and D.Q. performed the experiments. L.Li, P.N., and H.Z. supervised the experiments. B.T., H.Z., and P.N. conceived the project and co-wrote the manuscript.

Competing interests

The authors declare no competing interests.

Additional information

Supplementary information The online version contains supplementary material available at https://doi.org/10.1038/s41467-024-53196-3.

Correspondence and requests for materials should be addressed to Baolei Tang, Panče Naumov or Hongyu Zhang.

Peer review information *Nature Communications* thanks Junhui Jia, and the other anonymous reviewers for their contribution to the peer review of this work. A peer review file is available.